

Composition sensitivity of the Auger observatory through inclined showersM. Ave,¹ J. A. Hinton,^{1,2} R. A. Vázquez,³ A. A. Watson,¹ and E. Zas³¹ *Department of Physics and Astronomy, University of Leeds, Leeds LS2 9JT, United Kingdom*² *Enrico Fermi Institute, University of Chicago, 5640 Ellis Avenue, Chicago, Illinois 60637*³ *Departamento de Física de Partículas, Universidad de Santiago, 15706 Santiago de Compostela, Spain*

(Received 12 August 2002; published 28 February 2003)

We report a calculation of the expected rate of inclined air showers induced by ultra high-energy cosmic rays to be obtained by the Auger Southern Observatory assuming different mass compositions. We describe some features that can be used to distinguish photons at energies as high as 10^{20} eV. The discrimination of photons at such energies will help to test some models of the origin of ultrahigh-energy cosmic rays.

DOI: 10.1103/PhysRevD.67.043005

PACS number(s): 96.40.Pq, 96.40.Tv

I. INTRODUCTION

Uncovering the origin, composition and energy spectrum of the highest energy cosmic rays is one of the biggest challenges in astroparticle physics. The Pierre Auger project is the next step in the search for answers to intriguing questions about the origin of these particles [1]. The Auger Southern Observatory will consist of 1600 water Čerenkov detector stations (each $10\text{ m}^2 \times 1.2\text{ m}$ deep) on a triangular grid of 1500 m spacing overlooked by four detectors capable of detecting the fluorescent light emitted by the nitrogen molecules excited by the shower. The array covers a ground area of approximately 3000 km^2 at a mean altitude of 875 g cm^{-2} ($\sim 1400\text{ m}$), near Malargüe in Mendoza State, Argentina (latitude = -35.2° , longitude = -69.2°). The Auger Southern Observatory will be able to measure the energy of the incoming cosmic ray using fluorescent detectors (FD) and thus calibrate the estimates inferred from the surface detectors.

The proposal to use the Auger observatories to search for very inclined showers induced by ultrahigh-energy neutrinos [2] has led to an investigation of the characteristics of high-energy showers at large zenith angles (HAS), i.e. cosmic ray showers arriving at zenith angles larger than 60° [3].

They constitute the background to neutrino detection but their observation also provides a significant increase in the aperture of the array and may improve mass composition studies [4]. These showers would not be very different from vertical showers except for the fact that they develop in the upper part of the atmosphere. As a result the electromagnetic part of the shower, produced mainly from π^0 decay, is mostly absorbed well before the shower front reaches ground level.

In these showers the muon front propagates through the atmosphere and gets gradually attenuated through pair production, bremsstrahlung, and hadronic interactions that reduce the muon energy and increase their probability to decay in flight. The muon energy spectrum at ground has a *low energy cutoff* arising from muon decay which increases as

the zenith angle rises and the average muon energy at ground level also increases.¹

These energetic muons travel making small angles to the incoming cosmic ray direction and their trajectories are deflected by the Earth's magnetic field. As a result the muon density patterns at ground are very different from typical densities measured in vertical showers, the geomagnetic field acting as a kind of "natural magnetic spectrometer." The rate of inclined showers is governed by their muon content and is thus sensitive to primary composition. If the primary particles are photons, the showers that develop are muon poor and thus the inclined shower rate is much lower than for hadron primaries. Assuming that a mass independent energy spectrum can be measured otherwise, for example, using the fluorescence technique, inclined showers can provide stringent limits on photon abundance [4].

The Auger observatory will constrain photon composition above 10^{20} eV. This energy region is of particular interest because a number of models attempting to explain their origin predict large fractions of photons [5] and such measurements could be due to discrimination of these from other models.

This work outlines the sensitivity of the Auger Observatory to inclined air showers induced by ordinary cosmic rays. It predicts the expected shower rates for zenith angles above 60° assuming different primary mass compositions: proton, iron and photons.

The paper is organized as follows: in Sec. II we describe the procedure to calculate the expected rate for the Auger array above 60° for primary protons, giving the inclined shower rate as a function of shower energy for a reference flux and the expected values for the energy resolution, core error reconstruction, and multiplicity of stations as a function of the energy; a more detailed explanation of the procedure can also be found in [3]; in Sec. II we describe the effect of

¹The bulk of the overall increase in the average muon energy as the zenith angle rises is due to the increasing cutoff, but there is a small contribution due to the rise of the pion critical energy (the energy at which the pions are more likely to decay than to interact).

the geomagnetic interactions in inclined air showers initiated by photon primaries; in Sec. IV we present the expected rate for three primary mass compositions (protons, iron and photons). Finally in Sec. V we offer some conclusions.

II. SIMULATION OF INCLINED EVENTS AND THEIR ANALYSIS

The density patterns of inclined showers at ground level depend on energy, mass composition and interaction model much as for vertical showers. In addition, they also depend on zenith and azimuth angles because of the effect of the Earth's magnetic field. The simulation and reconstruction of events which is presented here rely on the model of the muon density patterns produced by inclined showers under the influence of the geomagnetic field described in [6]. This model approximates the magnetic distortions of circular symmetric muon density patterns generated by simulation in the absence of magnetic effects and provides a simple and continuous description of the average muon density functions for different arrival directions. These functions simplify fitting procedures and allow the simulation of the expected sensitivity of the Auger Surface Array for showers with a zenith angle above 60° .

A. Muon densities

With the help of AIREs [7] (version 2.2.1) and the adopted hadronic model, libraries with average muon density maps for inclined showers have been generated. These libraries contain showers with zenith angles between 60° and 88° in steps of 2° and all azimuth angles in steps of 5° . All showers have a reference energy of 10^{19} eV and muon density profiles for different primary energies are obtained using an appropriate scaling factor which has been shown to depend on the primary composition and the hadronic model considered [8]. In this work QGSJET98 [9] is used as the high-energy hadronic interaction model. The magnetic field at Malargüe, the site of the Southern Auger Observatory, has been taken to have an intensity $B=26 \mu\text{T}$ and an inclination of $I = -33.18^\circ$ (pointing in the upward direction). A northern site with a larger intensity and higher inclination would have a different distortion pattern and results can be expected to be somewhat different particularly in relation to azimuthal angle distributions.

Assuming an isotropic cosmic ray distribution consisting of protons and a given parametrization of its energy spectrum, the arrival of cosmic rays is simulated. A sub-array containing 91 detectors arranged in five concentric hexagons is considered and showers are assumed to have random impact points in the central region to save computing time. Inclined showers in the water Čerenkov tanks are dominated by muons. Using the muon density libraries the average number of muons expected at each tank position for each shower is calculated and the nearest integer number of muons is selected.

B. Tank signals

The signals for very inclined muons in water Čerenkov tanks can be greatly enhanced by direct light and muon interactions as has been shown in [8] for Haverah Park detectors. To account for the detector response to muons of different energies and angles of incidence, the WTANK [10] program based on the CERN GEANT package [11] has been used. For each artificial event, the expected numbers of muons at each detector are fluctuated according to the Poisson fluctuations, and the tank signals are also sampled according to the distributions of light fluctuations in the tank. These zenith angle dependent distributions include the response to the geometry of the muon tracks, the direct light contribution, and the catastrophic muon energy losses, namely hard bremsstrahlung, pair production or hadronic interactions, all of which become more important as the average muon energy rises, as obtained in the detailed numerical simulations using WTANK.

Simulations of inclined showers have shown that there is an electromagnetic component which is mainly due to muon decay in flight before the shower reaches the surface. This contribution represents a small fraction of about 20% of the signal in the tank produced by the muons themselves. This enhancement of the signal is considered as a fixed percentage of the muon signal. An electromagnetic component is also expected from π^0 decay in the showering process that takes place in a higher region of the atmosphere compared to vertical showers. This component is taken from simulations and treated as an additional correction to the tank signals. The simulations made indicate that the correction is small for zenith angles above 60° and confined to a relatively small region enclosed by a circle of radius ~ 500 m centered at the shower axis. It is neglected for zenith angles above 70° .

C. Event reconstruction

Artificial events have been generated in the energy range $10^{18.5}-10^{21}$ eV and in the zenith angle range $60^\circ-89^\circ$. We have assumed a simple trigger condition demanding 5 stations with a density greater than 0.4 vertical equivalent muons (VEM) m^{-2} . Following the steps of [3,4] the shower parameters of these artificial events (θ , ϕ , impact point position, and energy) are reconstructed as if they were real data. The procedure is based on a two-step fitting process using a maximum likelihood method which is iterated. Stations with densities below threshold are taken into account in the fitting procedure. The arrival direction angles are first fitted to the signal times in the "triggered" detectors and then the energy and impact point are varied to make the average muon density map fit the actual "measured" densities in the tank. Curvature corrections to the arrival times are implemented once there is an estimate of the core location: the process is iterated three times for convergence.

An example of a reconstructed event in the plane perpendicular to the shower direction is shown in Fig. 1, together with the contours of densities that best fit the data. In the figure the array is rotated in the shower plane such that the y-axis is aligned with the component of the magnetic field perpendicular to the shower axis. The asymmetry in the den-

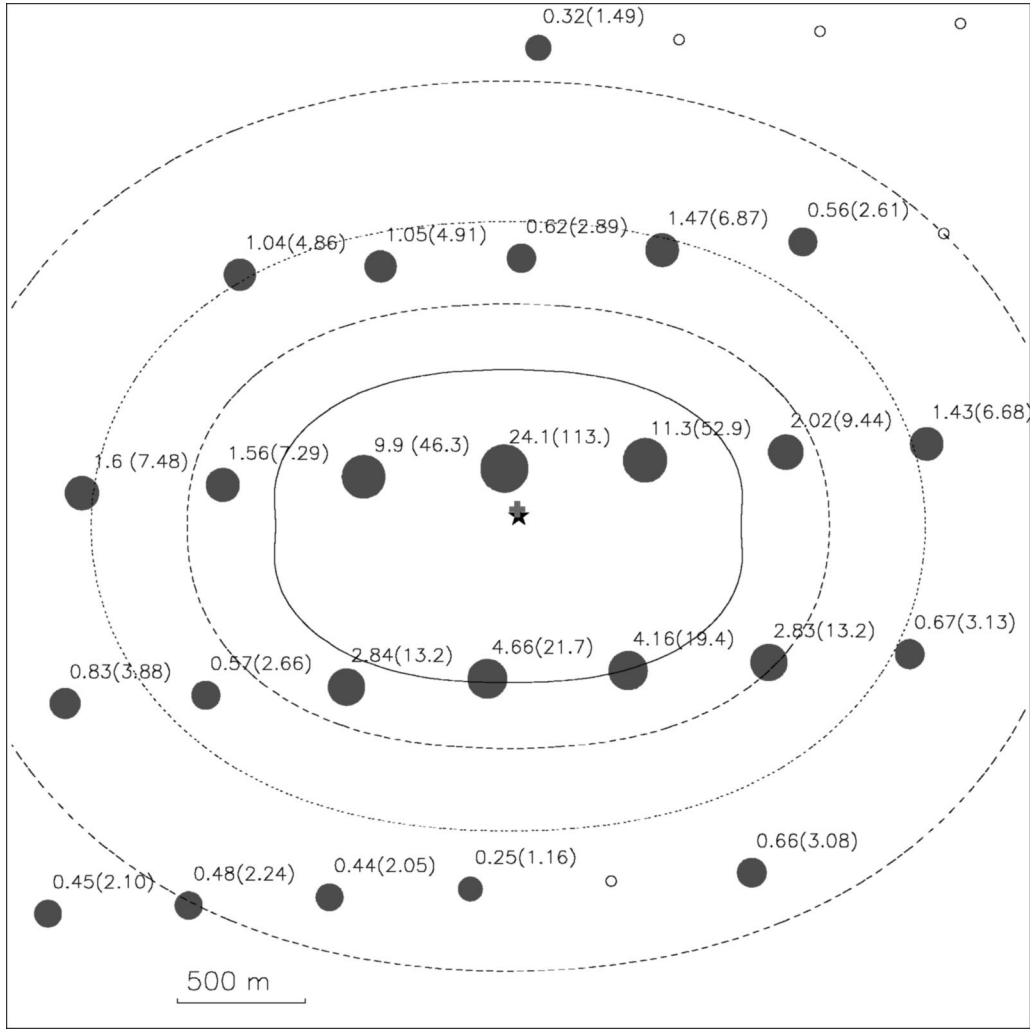


FIG. 1. Density map of a proton simulated event of $10^{19.52}$ eV at a zenith angle of 77° in the plane perpendicular to the shower axis. Recorded muon densities are shown as circles with radii proportional to the logarithm of the density. The positions of the best-fit and simulated impact points are indicated by a star and a cross, respectively. Densities in VEM m^{-2} are marked and, in brackets, the actual number of inclined muons that produced each signal. The y-axis is aligned with the component of the magnetic field perpendicular to the shower axis. Contour levels for 2, 5, 10 and 20 muons per station are shown for the fit. Detectors not triggered are indicated by an empty circle. The reconstructed energy and zenith angle are $\log_{10}(E/eV) = 19.6 \pm 0.06$ and $\theta = 76.5^\circ \pm 0.3$.

sity pattern due to the geomagnetic field is apparent. As anticipated [2], in spite of a relatively moderate energy, common events can be rather spectacular having over 20 tanks triggered.

We have estimated the detection rate as a function of primary energy integrating over all zenith and azimuth angles, assuming the parametrizations of the energy spectrum given in Ref. [12]. This parametrization is used for reference and lies between the energy spectra recently reported by the AGASA group [13] and the HiRes group [14]. For self-consistency, the energy spectrum to be used in a practical application of the ideas outlined here should be the one derived from the Auger experiment using the fluorescence technique, as the spectrum derived by this technique has the advantage of being independent of assumptions of primary mass composition.

D. Results

Results obtained in the simulated sub-array have been scaled up to the total array surface of 3000 km^2 . This approximate approach has two important implications. The sub-array “radii” range between $r_{sub} \sim 6.5$ and 7.5 km . This implies that in the transverse plane the maximum distance to shower axis is $r_{sub} \cos \theta$ which can be rather small for high zenith angles (for example, for a zenith of 75° the sub-array stops sampling at about 1.8 km). As a result the number of tanks that have a signal in the real Auger array will be severely underestimated for high zenith and high-energy showers. More tanks will help the reconstruction and can probably reduce the uncertainties so that our conclusions are conservative in that respect. Another implication is that no edge effects are taken into consideration but this is not expected to affect either the shower rate, or most of our results very

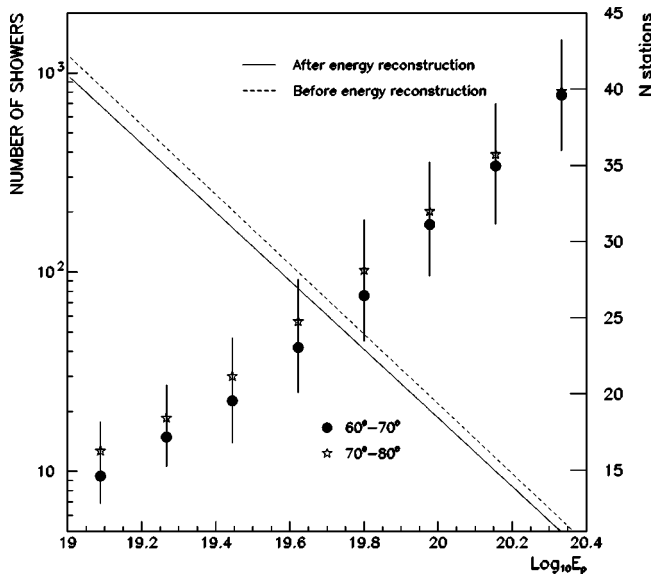


FIG. 2. Integral spectrum of events per year that trigger the Auger surface array, before and after energy reconstruction, assuming proton composition and adopting QGSJET as the high-energy interaction model. The Nagano and Watson flux has been assumed in this plot. The average multiplicity in the number of stations above threshold and its spread is also shown for two ranges in the arrival zenith angle, indicating that the multiplicity is increasing as the zenith rises. Hardly any reduction is observed at high energies. This is an artificial effect because of the limited number of stations simulated. Because we are using a reduced sub-array, the tank multiplicity given here should be considered as a lower bound (see text).

much, because a large fraction of the showers will fall well within the array.

Results are shown in Fig. 2. The dashed line is the integral rate that could be expected in a 3000 km² array from the cosmic ray spectrum from [12]. The continuous line represents the reconstructed spectrum. Quality cuts to the reconstructed events have been implemented, namely the downward error in the energy has been required to be less than 60% and the χ^2 probability for the energy and time fits have been forced to be greater than 1% for the accepted events. The difference in normalization, which amounts to $\sim 20\%$, is due to the combined effect of the quality cuts, systematic effects, fluctuations and the effect of the finite energy resolution of the detector. The number of events expected per year is ~ 1000 above 10^{19} eV and ~ 18 above 10^{20} eV after making these quality cuts, assuming a pure proton composition and the flux given in [12].

The multiplicity of detectors with a signal above 0.4 VEM m⁻² as a function of energy for the range of angles simulated is also shown in Fig. 2. For a given energy the multiplicity is much larger than for vertical showers. Two factors contribute to this effect: the reduction of the effective spacing between stations in the shower plane, and the flatter density profile of horizontal air showers compared to vertical.

As a shower becomes inclined the earliest and latest tanks that are above threshold can be quite far apart corresponding

to different depths in shower development. Due to the additional atmosphere traversed an attenuation can be expected for the late arriving particles. This was studied for muon distributions which are the dominant component in inclined showers in [6,15] and for electron distributions in [16]. If the number density of muons changes significantly over such a distance it can represent a significant correction to the densities derived in our work. It should be remarked that no attenuation of the shower particles across the array has been taken into account. As shown in [6], such attenuation effects become important at extreme zenith angles $> 87^\circ$, but for most of the zenith angle interval discussed in this paper the attenuation, which is less important than in the vertical case, can be ignored in a first approximation. As an example, simulations show that for a 30° shower, water Cerenkov density at 1000 m from the shower core in the shower plane is attenuated by a $\approx 30\%$ when reaching ground level. At 70° this factor is less than 15%. The main reason for this is that in the vertical direction the signal is dominated by electromagnetic particles from π^0 decay, while in the horizontal direction the signal at ground level is dominated by high-energy muons and secondary electromagnetic particles from decaying muons. The scale of the attenuation is roughly determined by the interaction length, which for photons and electrons is orders of magnitude smaller than that for muons.

We should also point out that in spite of using average density maps, statistical fluctuations of the shower densities are considered in this work. These are complicated effects that include fluctuations in the ratios of energy transported by charged and neutral pions in the hadronic interactions as well as fluctuations in depth of maximum. As obtained in simulations it typically represents a 20% effect on the overall muon number density normalization for proton primaries and it is rather independent of primary energy [3]. Much of the fluctuation corresponds to the first interaction. In the left panel of Fig. 3 we show the energy resolution for two energy ranges. Two factors contribute to the energy resolution calculated in this work: the variation of the number of muons at ground due to shower to shower fluctuations ($\approx 20\%$ for all energies) and the muon size reconstruction error (which evolves from 20% at 10^{19} eV to 10% at 10^{20} eV). Hence, at 10^{20} eV the energy resolution is dominated by shower to shower fluctuations. The errors in the reconstruction of the impact points of the analyzed events are also shown in Fig. 3. As an example it is ~ 70 m at 60° and it has a small variation with zenith angle due to the different effective spacing of the detectors when projected on to the transverse shower plane.

III. INCLINED SHOWERS INDUCED BY PRIMARY PHOTONS

The recent analysis of inclined data obtained at Haverah Park has opened a new window to establishing bounds on photon composition at ultrahigh energies [4]. As photon showers have far fewer muons than hadron showers, the expected rate of inclined showers created by photons detected with a surface array is reduced relative to the rate from protons or nuclei primaries. This is because the detection of

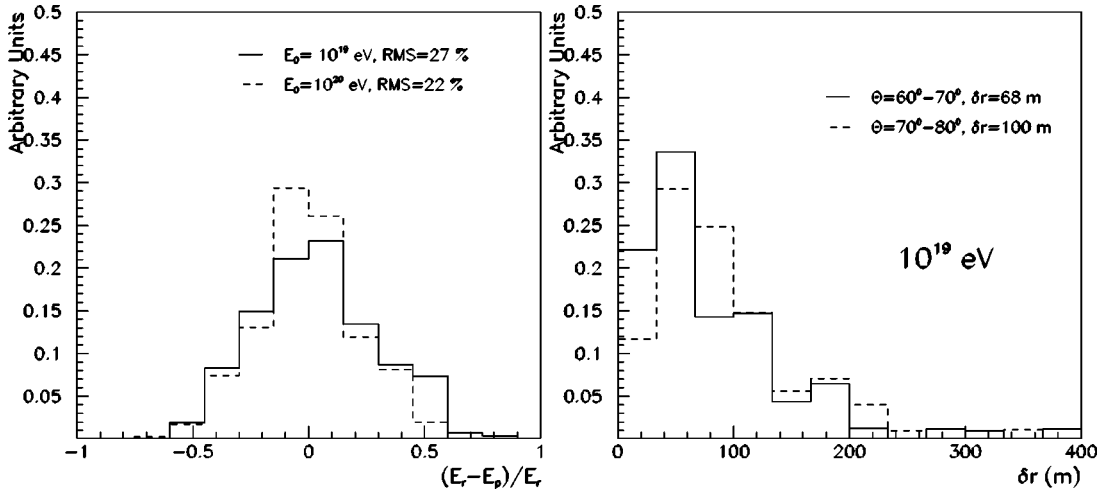


FIG. 3. Left panel: energy resolution integrated for all zenith angles in two energy bins. Right panel: distribution of the difference between the real and the reconstructed impact point positions in the energy range $10^{19.5} - 10^{20}$ eV for two zenith angle ranges.

horizontal showers induced by photons and hadrons by surface detectors is practically only sensitive to the muon component. The determination of the spectrum of cosmic rays through vertical shower measurements using the fluorescence technique, which is fairly independent of the primary composition, together with the inclined shower rate thus allow measurements of composition [3,4].

Following a similar procedure to that described in the previous section we now obtain the predicted integral spectrum for photon primaries for the Auger Observatories. There are a number of potential problems that could compromise the capabilities of the Auger Observatories to establish bounds or measure photon composition through inclined event rates, namely the Landau-Pomeranchuk-Migdal [17] effect, the rise in the photoproduction cross section [18] and the interactions of photons with the geomagnetic field of the Earth [19–21]. We discuss these effects in detail to show to what extent it can be expected that the Auger detector will be sensitive to photon primaries.

A. General features of inclined photon showers

The dominant process for muon production in an electromagnetic cascade is photoproduction:

$$\gamma + \text{nucleus} \rightarrow \text{hadrons}. \quad (1)$$

When photoproduction occurs the reaction products are essentially like those of a pion-nucleus interaction. Muons originate from the decay of the produced pions and kaons and their progeny in the resulting hadronic subshowers. The cross section for photoproduction has been measured up to $\sim 10^4$ GeV [22,23] for the incident photons in the laboratory frame. Above the resonance region (see Fig. 4) the cross section is about $100 \mu\text{b}$ per nucleon, and rises slowly for photon energies above ~ 10 GeV. The corresponding cross section on an air nucleus is ~ 1.1 mb, obtained by scaling $\sigma_{\gamma A} \sim A^\alpha \sigma_{\gamma p}$ where $\alpha \sim 0.9$. The ratio of the pair production to the photohadronic cross section gives the probability of a hadronic interaction to occur. This ratio is at 10 GeV:

$$R = \frac{\sigma_{\gamma \rightarrow \text{hadrons}}}{\sigma_{\gamma \rightarrow e^+ e^-}} \sim 2.8 \times 10^{-3}. \quad (2)$$

The ratio grows with the incident photon energy because of the rise in the photoproduction cross section, and it is expected to be $\sim 10^{-2}$ at 10^{19} eV. Figure 4 shows the measured photoproduction cross sections as a function of energy, together with the standard parametrization used by the AIRES code [7] and a recent parametrization given by Block *et al.* [18] from a combined analysis of pp , $p\gamma$ and $\gamma\gamma$ interactions.

As pointed out in Ref. [18], the photoproduction cross section is close to the saturation limit at DESY ep collider HERA energies and cannot grow with energy faster than the currently used parametrizations. Therefore, the Block *et al.* parametrization may be considered as an upper limit to the photoproduction cross section. Other potential sources of

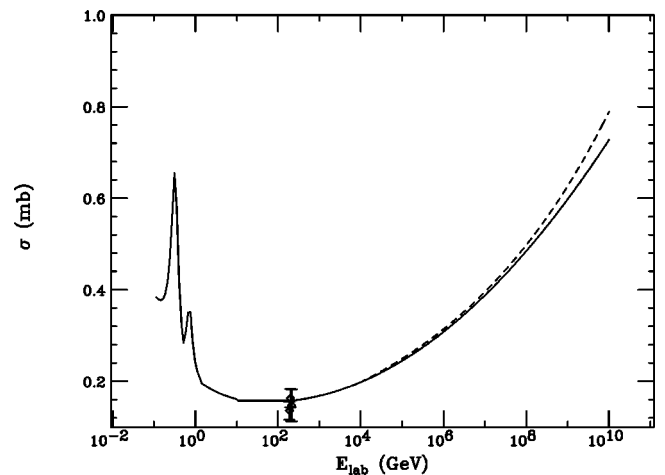


FIG. 4. Photon-proton photoproduction cross section as a function of the photon energy. The continuous line represents the parametrization of the AIRES code. The dotted line is the Block *et al.* parametrization [18]. Both curves are normalized at low energy. Points show data from HERA [22,23].

muons are smaller than this. Muon pair production, in which a pair of electrons is replaced by a pair of muons, is suppressed by a factor $m_e^2/m_\mu^2 \sim 2 \times 10^{-5}$ [24]. Hadron production by electrons also contributes less than photoproduction because the process has to occur through exchange of a virtual photon, and the energies of the produced hadrons are small.

The probability of photoproduction versus pair production is further enhanced at high energies when the Landau-Pomeranchuk-Migdal (LPM) effect takes place [17]. The LPM effect is a collective effect of the electric potential of several atoms and it tends to suppress the pair-production and bremsstrahlung cross sections for energies above a given value E_{LPM} , which is inversely proportional to the medium density. It starts to become relevant for the development of photon induced air showers at primary energies above 10^{19} eV for vertical showers [25], a value somewhat above E_{LPM} . This energy rises for large zenith angles corresponding to shower development higher up in the atmosphere where the air is thinner. We have found from simulations using the AIRES code that for the zenith angle range being discussed, the LPM effect has a mild impact on the total number of muons produced by photon showers (<25% at a zenith angle of 60°).

It has been pointed out before that the number of muons produced by a proton and iron primary rises with energy according to a simple scaling law [3] to a very good approximation:

$$N_\mu = N_0 (E/10^{19})^\beta, \quad (3)$$

where N_0 (the normalization, here taken at 10^{19} eV) and β (a constant parameter of order 0.9) are fixed numbers for a given zenith angle, hadronic interaction model and mass composition. The approximation is also valid for photon primaries although a number of differences are worth a brief discussion.

Batches of 100 photon-induced air showers using the AIRES code have been simulated at different zenith angles and energies, in the absence of magnetic field, using the two different extrapolations of the photoproduction cross sections which are shown in Fig. 4, namely the standard parametrization of AIRES and the parametrization of Ref. [18]. In Fig. 5 we plot the average number of muons generated by a photon as a function of energy for different zenith angles as obtained in the simulation. We note that the absolute number of muons of a photon shower is less than that of a hadron shower as expected from the ratio of probabilities in Eq. (2). However, the number of muons in a photon-induced shower rises with energy faster than in a proton shower so that differences between the two become smaller as the energy rises. This is also qualitatively expected from the behavior of the photoproduction cross section with energy. We also show for comparison an approximate scaling law using $\beta=1.2$ which we have used before as a conservative estimate [3,4].

In Fig. 5 a steepening kink of the curve at the highest energies can be noticed. This is due to the LPM effect which makes the showers develop deeper and further enhances the ratio R . The rise in R is a potential problem for the method.

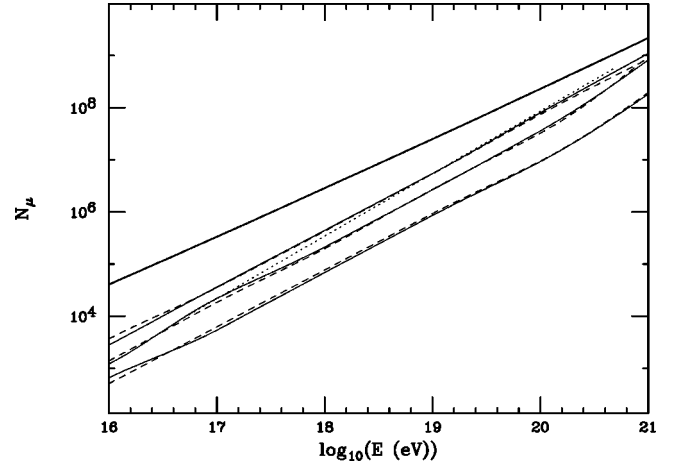


FIG. 5. Number of muons produced in inclined showers as a function of primary energy for proton showers (upper continuous line) and photon showers for 60° , 70° , and 80° , from top to bottom, using the standard AIRES parametrization (continuous) and the Block *et al.* parametrization (dashed). Also shown for $\theta=60^\circ$ is the $\beta=1.2$ parametrization used in our previous work (dotted line).

If the average number of muons in a photon shower becomes sufficiently close to that of a proton shower, no conclusion could be extracted regarding photon composition since a photon shower that photoproduces in the first interaction is practically indistinguishable from a proton shower of the same energy.

On the other hand, the difference in the number of muons produced for the two parametrizations used for the photoproduction cross section is small, which gives an idea of the uncertainty involved in this calculation (see Fig. 5). This is not surprising since it is clear that the number of muons in a photon shower is dominated by processes at lower energies closer to the region where data constrain the cross section.

Fluctuations in the number of muons in photon-induced showers are rather different from ordinary cosmic ray showers. If the first interaction of the incident photon happens to be hadronic (probability $R \sim 0.01$ at 10^{19} eV) then the shower is indistinguishable from a hadronic shower. The distribution for the total number of muons in a photon shower can thus be expected to have a long tail in the region of showers with a large number of muons, close to those of a proton shower. These non-Gaussian tails can affect the detection rates and for that reason we have implemented fluctuations in the number of muons in the photon shower using the distributions obtained in the simulations.

B. Interactions with the geomagnetic field

It was pointed out in [19–21] that photons above 10^{19} eV have a large probability to convert into an electron-positron pair in the presence of the Earth's magnetic field before entering the atmosphere. The strength of this interaction depends on EB_\perp where E is the photon energy and B_\perp is the transverse magnetic field. Therefore the probability of interaction will depend on the direction of the incoming photon with respect to the Earth's frame. For a given zenith angle it is a maximum when the photon trajectory intercepts the

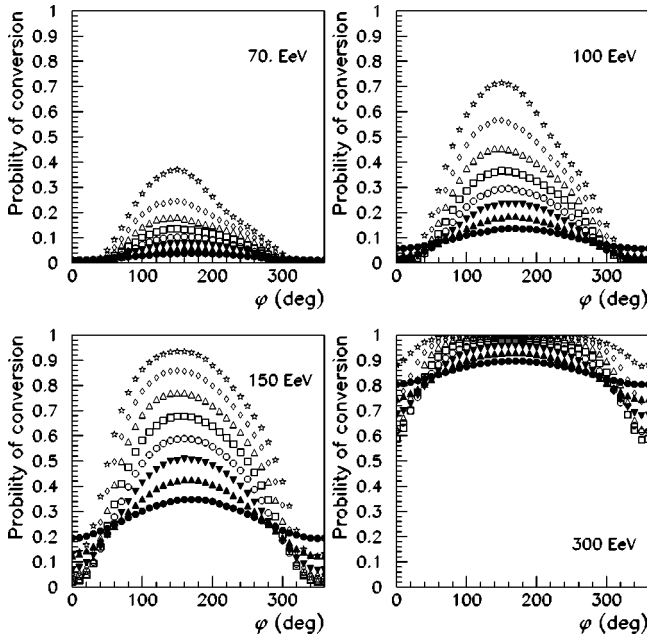


FIG. 6. Probability of photon conversion in the geomagnetic field as a function of azimuth angle for four different energies and eight different zenith angles. In each graph the eight curves are displayed corresponding, from bottom to top, to zenith angles from 10° to 80° in steps of 10° . An azimuth angle of 0° corresponds to a photon arriving from the geomagnetic north.

Earth's magnetic axis, which roughly corresponds to the geomagnetic south at the Malargüe site. This is because at a given distance to the center of the Earth the dipole field is strongest along the magnetic axis. For the same reason it is clear that the field will be largest for higher zenith angles. This azimuthal asymmetry was also pointed out by Stanev and Vankov [20] and by Bertou *et al.* [21] to be an alternative way to establish the high photon contribution (around 10^{20} eV).

The novel point that we want to make is that this interaction reduces the potential problems that could arise because of the increase in the photoproduction cross section and therefore “safeguards” the method of using the inclined shower rate for composition studies also for the highest energies. If such an interaction is deemed to happen an electron-positron pair is created that will radiate strongly by synchrotron radiation. A large number of photons is thus produced and some of them may give secondary pairs provided they still have sufficient energy. Instead of a single particle entering the upper atmosphere we end up with a spectrum of gammas and one or a few electron positron pairs adding up to the primary photon energy.

To study this effect a Monte Carlo program has been devised to simulate the cascading of photons in the geomagnetic field. The photon is injected at 20 000 km from the top of the atmosphere along the incoming direction and tracked in steps of 100 km. The values of the interaction length for pair production are taken from [26]. Figure 6 shows the probability of conversion for photons at different energies, zenith and azimuth angles. When a photon is converted, the resulting electron and positron are tracked in steps of 2 km,

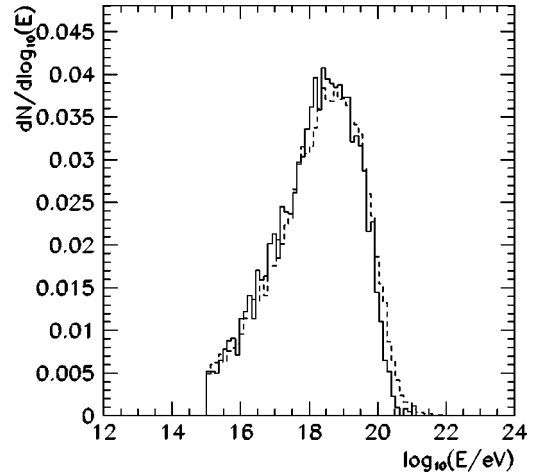


FIG. 7. Differential energy spectrum of electromagnetic particles resulting from the cascading in the geomagnetic field of primary photons at two different primary energies 10^{21} eV (continuous) and 10^{22} eV (dashed).

and the number and energy of the photons emitted via synchrotron radiation is calculated using the spectral distribution in [26]. The photons produced by magnetic bremsstrahlung are tracked and the probability of conversion calculated in each step. In this way, the spectrum of electrons, positrons and gammas at the top of the atmosphere can be obtained.

The relevant parameter for the inclined shower rate is the total number of muons in the shower. When the photon converts in the magnetic field, the number of muons at ground will be given by a sum over the contribution of the corresponding particle distribution:

$$N_\mu = \sum_i N_0 (E_i/10^{19})^\beta, \quad (4)$$

where E_i is the energy of particle i . Meanwhile for a photon that does not convert it is given by Eq. (3). Since the slope parameter in this equation, β , is greater than one the number of muons is reduced when the photon interacts with the Earth's magnetic field relative to when it does not.

It is of some interest to comment on a few facts about this conversion process. The strength of the Earth's magnetic field is such that efficient conversion starts at energies of order 10^{20} eV. Figure 6 illustrates how at energies of about 3×10^{20} eV the conversion probability is close to one, and this results in a relatively sharp cutoff. It is remarkable that at large energy the shape of the resulting spectrum does not depend much on the primary photon energy as can be seen in Fig. 7. The spectrum reflects mainly the spectrum of magnetic bremsstrahlung as the electrons and positrons produced travel and loose energy. It has a peak at about 10^{19} eV given by the strength of the magnetic field at the top of the atmosphere. The two energy features of the resulting spectrum, namely the cutoff and the peak, both scale with a negative power of the magnetic field strength at the detector location.

When the photon energy is well above the cutoff energy it gives rise to a sort of universal photon spectrum, its shape is independent of the primary energy and only mildly depen-

dent on the arrival direction; only the total number of particles changes. The final spectrum can be parametrized by

$$\frac{dN_{em}}{d\log E} = k \left[\frac{E}{E_c} \right]^\gamma \left[1 + \frac{E}{E_c} \right]^\delta, \quad (5)$$

where for the Malargüe site $\gamma=0.24$, $\delta=-1.7$, $E_c = 10^{19.76}$ eV, and k is a normalization constant which due to energy conservation scales linearly with the primary photon energy. This linear relation implies that when the photons convert, we can talk, equivalently, about an effective slope parameter of $\beta_{\text{eff}}=1$ [in Eq. (3)].

At this point the method described in the previous section can be used to generate artificial events on the Auger array. We use the conversion probability for the photon showers to predict their behavior. These events are then reconstructed as if they were protons, and an equivalent energy (E_p) is calculated.

It is interesting to note that, coincidentally, the energy at which photon conversion becomes efficient is also that at which the LPM effects start to show up in shower development, $\approx 10^{19}$ eV [25] for a vertical air shower. When a photon is converted, it is seen from the spectrum shown in Fig. 7, most of the particles that will reach the top of the atmosphere and initiate the shower will be below the LPM threshold. The magnetic field of the Earth shields the atmosphere and the probability that showers develop in the atmosphere with strong LPM suppression becomes very small. The effective shielding is strongest at high zenith angles because the energy at which the LPM effect starts to take up is higher.

This is fortunate because, as Fig. 5 shows, if a high energy photon reaches the top of the atmosphere, the number of muons produced in the corresponding shower could become rather large and close to that of proton induced showers.

IV. COMPOSITION ANALYSIS WITH HAS

In Fig. 8 the integral energy spectra obtained from the artificial events is shown under three different assumptions for the primary composition (protons, iron, and photons) and using the cosmic ray parametrization given in [12]. The rate expected in the case of protons for a parametrization of the HiRes data [14] is also shown and can be considered as a lower bound if the primaries are protons. The hybrid character of the Auger Observatory is of utmost importance in the resolution of the flux controversy, and that should come in the near future.

In all the cases the artificial events are generated with muon density maps obtained for each specific primary, and then reconstructed as if they were protons, obtaining an equivalent energy (E_p). For primary photons, calculations are done using the Block *et al.* photoproduction cross section and also using an approximate parametrization for the number of muons in photon showers conservatively consistent with AIREs simulations, as discussed in [4], which amounts to using a value of $\beta=1.2$ in Eq. (3). The spectra are calculated switching on and off the interaction with the geomagnetic field for each of the two cases considered.

Three important features are clear in this picture:

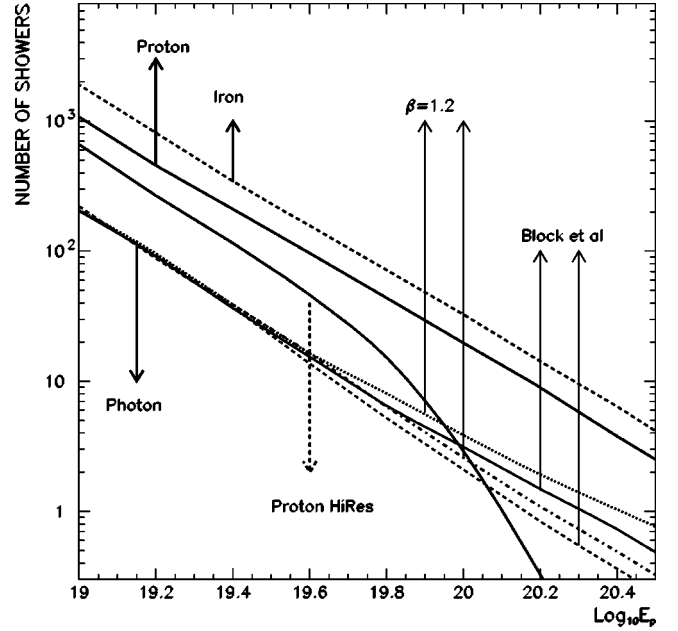


FIG. 8. Integral E_p spectrum of events per year triggering the Auger surface array ($\theta > 60^\circ$) for three assumptions of primary composition using the Nagano and Watson parametrization. For photons two sets of spectra are calculated corresponding to the two different assumptions about the rise with energy of the number of muons produced in photon showers. In each set the upper spectrum corresponds to photons neglecting interactions in the geomagnetic field of the earth and the lower spectrum gives the result taking into account this effect as described in the text. The curve marked as HiRes shows the prediction obtained for proton primaries taking a parametrization of the cosmic ray flux as measured by the HiRes collaboration.

The expected rate for primary photons above 10^{20} eV is reduced 30% when geomagnetic interactions are taken into account.

The two photoproduction cross sections used predict a rate for photon primaries ~ 10 times smaller compared to the predictions for other hadronic primaries.

Geomagnetic interactions modify the slope of the spectrum for primary photons at energies above $10^{19.6}$ eV.

Because of the geomagnetic effect the uncertainty on the photoproduction cross sections at high energies has a small effect on the muon number at ground level. The predicted distortion of the longitudinal shower development for photon primaries because of the LPM effect is reduced because of the geomagnetic interactions. Assuming that the vertical flux is well measured independently of mass composition, as expected to be achieved with a fluorescence detector, the rate of inclined showers could be used to impose strong constraints on primary photon composition assuming a given hadronic model.

The hadronic model uncertainty can change the normalization of the spectra shown in Fig. 8. Therefore this method is not adequate to impose constraints on both mass composition and hadronic models at the same time. It should be used in combination with vertical measurements on mass composition using the same hadronic model. However, the

differences in muon densities between the different hadronic models available are $\approx 40\%$ [27], which is comparable to the difference between densities produced by proton and iron primaries [28], and therefore, these primaries cannot be resolved by using the overall rate measurements. Nevertheless the difference between photon and hadronic primaries are much larger, a factor of 6 at 4×10^{20} eV, so that this method can, on its own, impose severe constraints on the photon content of the highest energy cosmic rays.

Currently the ultrahigh-energy data suggest a mostly hadronic composition [4,29], and the inclined showers rate is well described by proton primaries at energies above $\sim 10^{19}$ eV [4]. If there is a change of composition to a photon dominance at higher energies, the rate of inclined showers will be much lower than predicted here. After a few years of operation of the Auger Observatory these features will help to establish bounds on the flux of photons at energies as high as 10^{20} eV.

V. CONCLUSIONS

Inclined showers will be seen in the Auger Observatory as spectacular events with as many as 30 or 40 detectors hit. We have calculated the approximate rate of inclined showers with zenith angle exceeding 60° expected to be observed at the Pierre Auger Observatory. This rate increases the aperture of the observatory by almost a factor of 2. Assuming a pure proton composition, there will be about 1000 well reconstructed events above 10^{19} eV per year, with a mean energy error of $\sim 25\%$. The rate is sensitive to composition. If pho-

tons were dominant at high energy, the rate would be an order of magnitude smaller than if they were protons or nuclei allowing for a clear discrimination of the two cases. Uncertainties in the physics at very high energies have implications for our results on the detailed quantitative predictions but these uncertainties have little impact on the previous conclusions.

There are other signatures of the presence of photons (see, for instance, Ref. [21]). Surely the combination of the inclined shower rate measurements together with vertical flux determinations and detailed analysis of the expected photon signatures will be a great step in the establishment of the overall photon rate at very high energies with the forthcoming data from the Auger experiment [30].

ACKNOWLEDGMENTS

We thank F. Halzen, M. Teshima, and K. Shinozaki for discussions and P. Billoir and S. Sciutto for very useful comments after careful reading of the manuscript. We also thank F. Halzen for bringing up the issue of photoproduction uncertainty. This work was partly supported by the Xunta de Galicia (PGIDIT02 PXIC 20611PN), by MICYT (FPA 2001-3837 and FPA 2002-01161), by PPARC (PPA/9/5/1998/00453), by the European Science Foundation (ESF Scientific Network N-86), and by FEDER funds. The work of R.A.V. is supported by the "Ramón y Cajal" program. We thank the "Centro de Supercomputación de Galicia" (CESGA) for computer resources.

-
- [1] The Pierre Auger Collaboration, in *Proceedings of the XXVII International Cosmic Ray Conference, Hamburg* (Copernicus Gesellschaft, Katlenburg-Lindau, 2001), Vol. 1 pp. 699–763, www.auger.org.
 - [2] J. Capelle, J.W. Cronin, G. Parente, and E. Zas, *Astropart. Phys.* **8**, 321 (1998); G. Parente and E. Zas, in *Proceedings of the High Energy Neutrino Workshop*, edited By M. Baldo Ceolin, Venice, 1996.
 - [3] M. Ave, J.A. Hinton, R.A. Vázquez, A.A. Watson, and E. Zas, *Phys. Rev. D* **65**, 063007 (2002).
 - [4] M. Ave, J.A. Hinton, R.A. Vázquez, A.A. Watson, and E. Zas, *Phys. Rev. Lett.* **85**, 2244 (2000); astro-ph/0112071.
 - [5] P. Bhattacharjee and G. Sigl, *Phys. Rep.* **327**, 109 (2000); S. Sarkar and R. Toldra, *Nucl. Phys.* **B621**, 495 (2002); V. Berezhinsky and M. Kachelriess, *Phys. Rev. D* **63**, 034007 (2001); V. Berezhinsky, *Nucl. Phys. B (Proc. Suppl.)* **87**, 387 (2000); V. Berezhinsky, A. Vilenkin, and M. Kachelriess, *Phys. Rev. Lett.* **79**, 4302 (1997).
 - [6] M. Ave, R.A. Vázquez, and E. Zas, *Astropart. Phys.* **14**, 91 (2000).
 - [7] S.J. Sciutto, in *Proceedings of the XXVI International Cosmic Ray Conference Salt Lake City* (AIP, Melville, NY, 1999), Vol. 1, p. 411; S.J. Sciutto astro-ph/9911331.
 - [8] M. Ave, J.A. Hinton, R.A. Vázquez, A.A. Watson, and E. Zas, *Astropart. Phys.* **14**, 109 (2000).
 - [9] N. Kalmykov, S. Ostapchenko, and A.I. Pavlov, *Nucl. Phys.* **B552**, 17 (1997).
 - [10] J.R.T. de Mello Neto, WTANK: A GEANT Surface Array Simulation Program GAP note 1998-020.
 - [11] R. Brun *et al.*, GEANT, Detector Description and Simulation Tool, CERN, Program Library CERN (1993).
 - [12] M. Nagano and A.A. Watson, *Rev. Mod. Phys.* **72**, 689 (2000), and references therein.
 - [13] N. Sakaki *et al.*, in Ref. [1], p. 333.
 - [14] T. Abu-Zayyad *et al.*, astro-ph/0208301.
 - [15] M. Ave, L. Cazón, R.A. Vázquez, and E. Zas, in Ref. [1], p. 1175.
 - [16] M.T. Dova and A. Mariazzi, in Ref. [1], Vol. 2, p. 539.
 - [17] L. Landau and I. Pomeranchuk, *Dokl. Akad. Nauk SSSR* **92**, 535 (1953); **92**, 735 (1953); A.B. Migdal, *Phys. Rev.* **103**, 1811 (1956); *Sov. Phys. JETP* **5**, 527 (1957).
 - [18] M.M. Block, E.M. Gregores, F. Halzen, and G. Pancheri, *Phys. Rev. D* **60**, 054024 (1999); M.M. Block, F. Halzen, and G. Pancheri, *Eur. Phys. J. C* **23**, 329 (2002).
 - [19] B. McBreen and C.J. Lambert, *Phys. Rev. D* **24**, 2536 (1981).
 - [20] T. Stanev and H.P. Vankov, *Phys. Rev. D* **55**, 1365 (1997).
 - [21] X. Bertou, P. Billoir, and S. Dagoret-Campagne, *Astropart. Phys.* **14**, 121 (2000).
 - [22] H1 Collaboration, T. Ahmed *et al.*, *Phys. Lett. B* **299**, 374 (1993).

- [23] ZEUS Collaboration, M. Derrick *et al.*, Phys. Lett. B **293**, 465 (1992).
- [24] T.K. Gaisser, F. Halzen, T. Stanev, and E. Zas, Phys. Lett. B **243**, 444 (1990).
- [25] F.A. Aharonian, B.L. Kanevsk, and V.A. Sahakian, J. Phys. G **17**, 199 (1991); A.N. Cillis, H. Fanchiotti, C.A. Garcia Canal, and S.J. Sciutto, Phys. Rev. D **59**, 113012 (1999).
- [26] T. Erber, Rev. Mod. Phys. **38**, 626 (1966).
- [27] J. Alvarez-Muniz, R. Engel, T.K. Gaisser, J.A. Ortiz, and T. Stanev, Phys. Rev. D **66**, 033011 (2002).
- [28] T.K. Gaisser, *Cosmic Rays and Particle Physics* (Cambridge University Press, Cambridge, England, 1990).
- [29] K. Shinozaki *et al.*, in Ref. [1], Vol. 1, p. 346; K. Shinozaki *et al.*, Astrophys. J. Lett. **571**, L117 (2002).
- [30] See the Auger home page in the Southern Observatory, <http://www.auger.org.ar/CDAS/>